Green Chemistry

Accepted Manuscript

ROYAL SOCIETY OF CHEMISTRY

www.rsc.org/greenchem

A facile direct chemical synthesis of well disperse L1_0-FePt Nanoparticles with tunable coercivity and controlling size

Jianghai He, [1, §] Baoru Bian, [1, §] Qiang Zheng,[2] Juan Du,[1,*] Weixing Xia,[1] Jian Zhang, [1]Aru Yan, [1] J. Ping Liu[3]

[1]Key Laboratory of Magnetic Materials and Devices, Ningbo Institute of Material Technology & Engineering, Chinese Academy of Sciences, Ningbo 315201, China

[2] School of Materials Science and Engineering, Ningbo University of Technology, Ningbo, 315016, China

[3]Department of Physics, University of Texas at Arlington, Arlington, TX, United States.

[§]These authors contributed equally to this work.

***Corresponding author: dujuan@nimte.ac.cn (J.Du)**

Chemical ordered FePt ($L1_0$ or Face-centered tetragonal fct-FePt) nanoparticles (NPs) with large magnetocrystalline anisotropy are of great interest for different applications,[1] such as high density magnetic recording media,[2] high performance permanent magnets,[3] catalyst,[4] and biomedicine.[5] Green and concise preparation is the precondition of nanoparticle application. The control synthesis of FePt nanoparticles started from the year of 2000 when Sun and co-authors reported a chemical self-assemble method based on the reduction of mixed metal salts ($Fe(CO)_5$ and $Pt(acac)_2$) in the presence of a long chain carboxylic acid and primary amines in organic solvents,[2b] which has been widely adopted to synthesize FePt nanoparticles until now. But the synthesized FePt nanoparticles exhibit chemically disordered face centered cubic (fcc) structure, which has a very small magnetocrystalline anisotropy. High temperature (usually above 550°C) annealing is necessary to realize phase transformation from the fcc structure to the ordered fct/$L1_0$ structure. In the high temperature annealing process, nanoparticles agglomerate and the size distribution will be destroyed.[6] In order to prevent agglomeration, shell coating (e.g., MgO, SiO_2) was applied,[7] which needs more than three steps including synthesis of fcc-FePt nanoparticles, coating them to get FePt@MgO/SiO_2 core-shell particles, and removing of the shells. Although the coated shell can be removed in the subsequent process, which making the fcc to fct conversion very difficult and incomplete. Later on, a salt matrix method was developed.[8] But it still needs to synthesize fcc-FePt nanoparticles in solution environment first, also, which has limited yield and the yield will further reduce after removing of matrix. A modified solution method to direct synthesis of $L1_0$-FePt NPs has been recently reported, such as adding a third metal element (Au, Ag), which can reduce the ordering temperature to 400°C, but the fraction of the ordered phase is usually small.[9]

Compared with the method of solution phase synthesis of fcc-FePt nanoparticles followed by high temperature annealing to get $L1_0$-FePt nanoparticles, one step method attracts more attention. He and Zhao have developed a simple one step synthesis of $L1_0$-FePt NPs by simultaneous decomposition of $Fe(NO_3)_3\cdot9H_2O$, $H_2PtCl_6\cdot6H_2O$ and direct catalytic graphitization of a carbon precursor (citric acid) at high temperature in solid phase,[10] but the size of the particles was ultrasmall (mostly 2~4 nm) even sintered at temperature of 850°C for 2 hours, therefore the coercivity was just 4.56kOe. More recently, Hu and co-workers reported a solvent-free chemical synthesis of $L1_0$-FePt nanoparticles using the synthesized intermediate $[Fe(H_2O)_6]PtCl_6$ as metal precursors, which was then mixed with different ratio of NaCl before sintering.[11] For the obtained FePt nanoparticles, which can obtain chemical ordered phase at annealing temperatures as low as 400 ^{o}C due to the intermediate precursor itself has a certain chemical order, the coercivity can be as large as 10.9 kOe. In a certain degree, this method has much improvement, but it still needs at least two steps.

Here, we report a simple approach for large scale and direct synthesis of $L1_0$-FePt NPs with tunable coercivity and controlling size. Unlike the previously reported method, no organic solvents, surfactant, chelating agent/catalyst or intermediate precursors are used, and the composition of Fe and Pt is easy to control, which is essential to achieve L1_0-FePt phase. In our previous work,[12] uniform 14 nm FePt nanoparticles were synthesized on ultra-thin carbon film, and its growth mechanism was proposed and a schematic diagram was shown. In this work, a medium of NaCl particles was used to synthesize collectable FePt nanoparticles with large yield, tailored size and tuned coercivity depending on sintering temperatures. The L1_0-FePt NPs synthesized by this method exhibit ferromagnetic property with coercivity up to 21.5 kOe at room temperature. This work provides a unique method for preparing high temperature phase/chemical ordered nanoparticles with only one simple step. It can also be applied for fabrication of some nanostructure, which is difficult to realize in liquid environment.

The metallic precursors, platinum (II) acetylacetonate ($Pt(acac)_2$ 99.9%) and Fe(III) acetylacetonate ($Fe(acac)_3$ 99.9%) were purchased from Alfa Aesar China. All the reagents were used without further purification. For preparing L1_0-FePt NPs, 0.25 mmol $Pt(acac)_2$ and 0.25 mmol $Fe(acac)_3$ were mixed with NaCl (the weight ratio of the precursor and salt is 1: 500), and milled for 24 h. The size of the NaCl was about 3 μm. Then, the powder was heated (with a heating rate of 10 °C/min) up to a certain temperature (several synthesizing temperatures of 300 ^{o}C, 350 ^{o}C, 400 ^{o}C, 450 ^{o}C, 550 ^{o}C and 750 ^{o}C were set) in a tube furnace under a flow of 100sccm reducing atmosphere with 8% H_2 and 92% Ar. The samples were kept at synthesizing temperature for 1h. After cooling down, a black powder was collected, and washed with deionized water.

DTA and TG were measured to know the decomposition process of the mixture of precursors ($Fe(acac)_3$ and $Pt(acac)_2$) in an alumina crucible with a heating rate of 5 °C/min under Ar flow. X-ray diffraction (XRD) characterization was carried out on a Bruker AXS D8-Advanced diffractometer with Cu Kα radiation (λ = 1.5418 Å). High-resolution TEM (HRTEM) and the high angle annular dark-field scanning TEM (HAADF-STEM) images were obtained on FEI Tecnai F20 200 kV TEM. The composition of the particles was semi-quantitatively determined by energy dispersive X-ray spectroscopy (EDS). Selection area electron diffraction (SAD) was used for structure characterization. Magnetic properties were measured using a Magnetic Property Measurement System (SQUID MPMS).

The procedure of the synthesis $L1_0$-FePt nanoparticles is shown in **Figure 1**. The design of our experiment is to let Fe and Pt atoms nucleate and grow into FePt nanoparticles on a substrate and then the substrate is removed and nanoparticles are colleted. Here, $Fe(acac)_3$ and $Pt(acac)_2$ (acac = acetylacetonate) were chosen as precursors of Fe and Pt. NaCl was selected as the substrate, which has a high melting point of 801 °C. NaCl is a perfect option since it is easy to be ground down to small size and also easy be removed with deionized water after synthesizing. For synthesizing $L1_0$-FePt, NaCl particles can also work as insulation media preventing agglomeration during high temperature sintering.

The decomposition of $Fe(acac)_3$ and $Pt(acac)_2$ is $Pt(C_{10}H_{14}O_4)/Fe(C_{15}H_{21}O_6) \rightarrow Pt/Fe + H_2O + C$. In order to make it clear when the decomposition happened, DTA and TG were shown in Figure S1 (Supporting Information). From the weight loss curve, it can be seen that the decomposition happened from 200 °C, and endothermic peak has a little bit delay. Then the obtained metal atoms nucleate and grow on a substrate of NaCl. Several sintering temperatures were set to synthesize FePt nanoparticles.

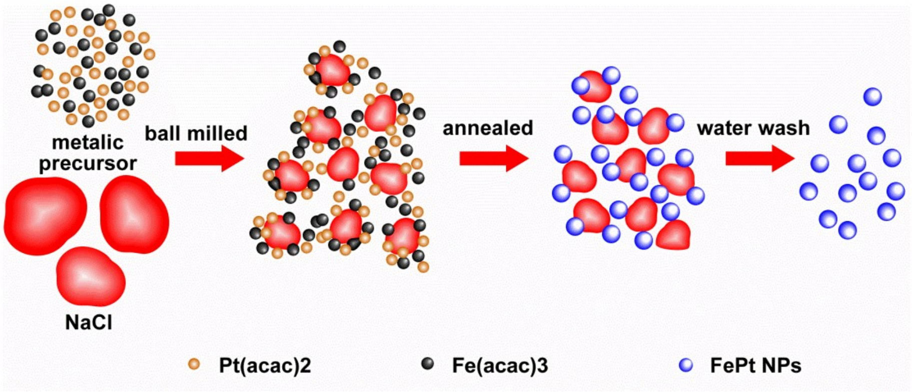

Figure 1. Schematic representation of the synthesizing of L1_0-FePt nanoparticles.

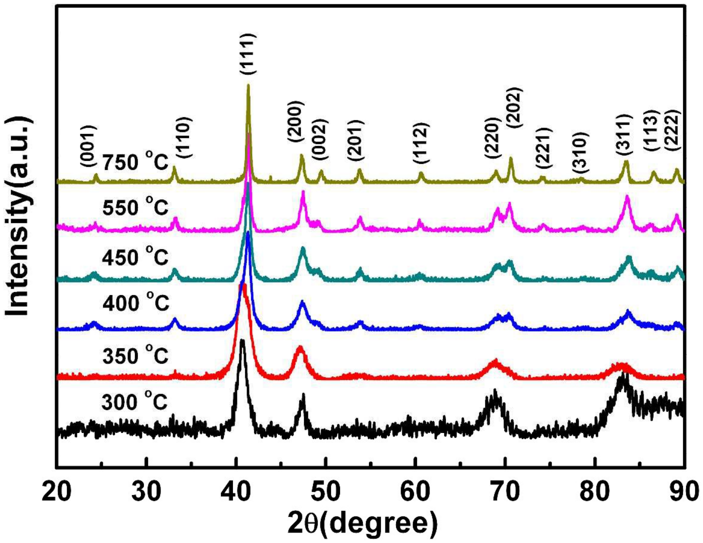

Figure 2. X-Ray diffraction patterns of the FePt nanoparticles prepared at 300 °C, 350 °C, 400 °C, 450 °C, 550 °C and 750 °C after removing the sodium chloride.

XRD patterns in **Figure 2** show the L1_0-FePt nanoparticles prepared at 300 °C, 350 °C, 400 °C, 450 °C, 550 °C and 750 °C after removing the sodium chloride. It can be seen that all NaCl peaks disappeared after simple water washing. No peaks corresponding to Pt or Fe are presented in the diffraction pattern. The particles prepared at 300 ^{o}C have fcc structure, and no (001) and (110) peaks are found, which are characteristic peaks for L1_0-FePt; while those of sintered at 350 ^{o}C have trivial peak of (110), which is almost undetectable. Therefore particles prepared at 300 ^{o}C almost have no coercivity (530 Oe) as shown in the supporting information in Figure S4, and those of 350 ^{o}C have a coercivity of 3.15 kOe, which will be shown in Figure 6. It can be clearly observed that more ordered L1_0 phase of the FePt nanoparticles has been successfully formed when the synthesizing temperature is up to 400 ^{o}C, when the characteristic superlattice peaks (001) and (110) of L1_0-FePt have much stronger intensity. The higher the sintering temperature, the stronger the characteristic peaks of L1_0-FePt phase. And all the peaks become sharper and narrower with increasing the sintering temperatures, which means the obtained nanoparticles have grown into larger ones. The average particle diameters estimated from Scherrer's formula for the particles prepared at different temperatures are 6.6 nm, 7.2 nm, 8.3 nm, 9.8 nm, 11.5 nm and 15 nm respectively, which were shown in Figure 3 with error bars. The mean size of the particles prepared at different temperatures was also listed in Table 1 in the supporting information. The following part will show TEM of the particles obtained at different synthesizing temperatures, in which the average particle size is consistent with that calculated by Scherrer formula from XRD.

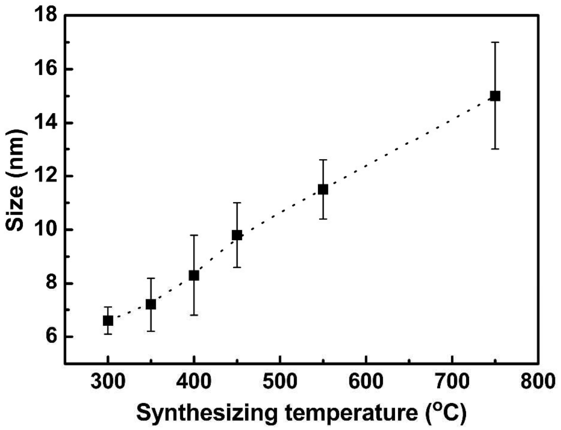

Figure 3. The average particle diameters of the particles prepared at different temperatures

As shown in Figure 2, the higher the sintering temperature, the stronger the characteristic peaks of $L1_0$-FePt phase. Since the magnetic properties such as coercivity of hard magnetic nanoparticles depend on both size and ordering degree. Here the degree of chemical ordering (S) of the $L1_0$ phase was quantified and calculated using the following equation: [13]

$$S \cong 0.85\left[\frac{I_{001}}{I_{002}}\right]^{1/2} \qquad (1)$$

where I_{001} and I_{002} are the intensities of (001) and (002) diffraction peaks from the XRD patterns. As expected, S increases with increasing of sintering temperature. The S of the particles prepared at 400 °C, 450 °C, 550 °C and 750 °C is 0.57, 0.64, 0.66, and 0.72, respectively. S was listed in **Table 1** in the supporting information. In the case of annealed at 300 °C and 350 °C, S can’t be calculated since no superlattice peaks of (001) and (002) can be found. The peak width decreases with the increasing of preparation temperature, indicating that the larger particle size formed.

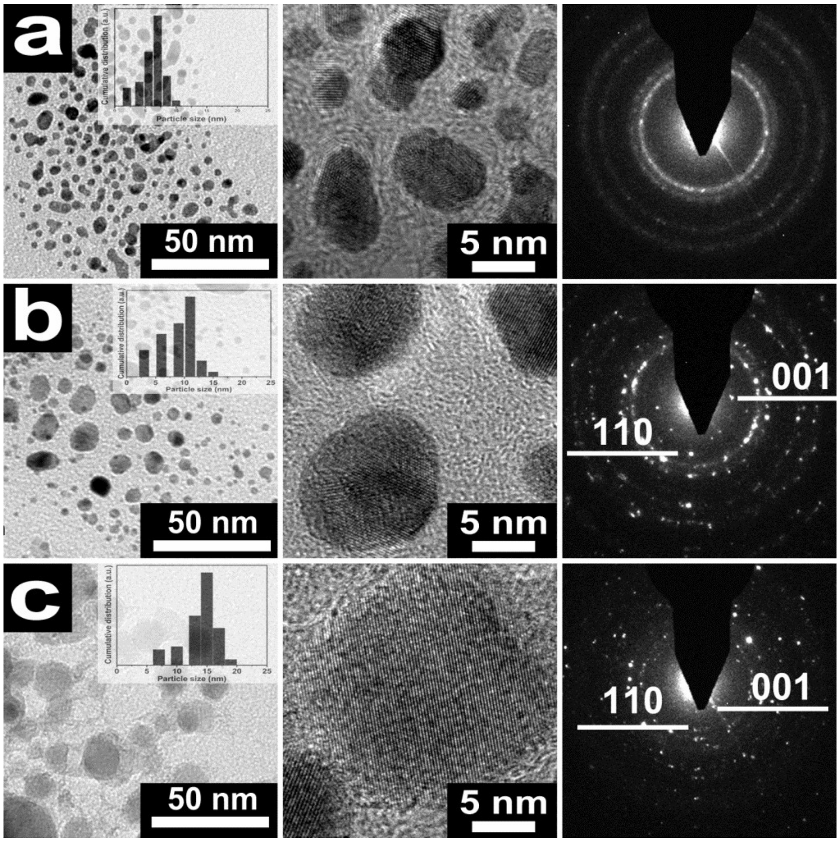

Figure 4. TEM, HRTEM and SAD images of the FePt NPs obtained at 350 °C (a), 550 °C (b), 750 °C (c). The insets show the size distribution of the particles. In each case, at least 300 particles were counted to determine the size and size dispersion.

From the TEM images of the synthesized FePt NPs at 350 ^{o}C, 550 ^{o}C and 750 ^{o}C (as shown in **Figure 4**) and 300 ^{o}C, 400 ^{o}C and 450 ^{o}C (shown in Figure S2, Supporting Information), all the particles have a good dispersion on TEM grid after sonication in alcohol, no coalesce was observed, which means that NaCl has played a perfect insulation effect during synthesizing process. The mean particle size measured in TEM is consistent with that calculated by XRD. For sample obtained at 350 ^{o}C, the bright-field images (**Figure 4**a) indicate a size distribution in the range of 2-10 nm (Figure 4a insert image), which has a mean size of 7.2 nm. All the observed NPs are mainly single crystals as shown by the high-resolution TEM (HRTEM) images. As shown in SAD image (in Figure 4a), the (100) and (110) characteristic superlattice rings was not clear, which indicated that the particles have not formed obvious fct structure. For sample obtained at 550°C, the bright-field images (**Figure 4**b) indicate that the size distribution was mainly in the range 5–14 nm with a mean size of 11.5 nm. There were also some particles smaller than 3nm. The (100) and (110) characteristic superlattice rings in the SAD pattern (Figure 4b) confirmed that the FePt NPs have fct structure. The majority of the NPs obtained at 750°C have a larger size in the range of 14–17 nm with a mean size of 15 nm, which has a very narrow size distribution as shown in **Figure 4**c. Very few NPs larger than 20 nm or smaller than 5nm were observed. The HRTEM images confirm the presence of single crystal NPs, and SAD patterns confirmed the fct structure. The coincidence of the particles size measured from TEM with that of calculated from XRD further proves the synthesized FePt nanoparticles have single crystal structure. At temperatures higher than the decomposition of metal precursors, nanoparticles can be synthesized. The higher the sintering temperature is, the larger the particle's size can be acquired; the lower the sintering temperature is, the finer the particles can be obtained. It should be noticed that a coating of carbon is observed on the synthesized FePt nanoparticles in Fig.4c which comes from the decomposition of metal precursors.

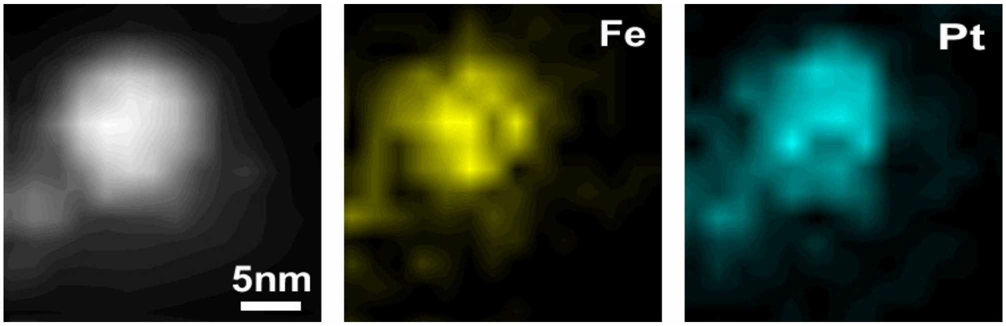

Figure 5. HAADF image and the corresponding elemental map of FePt NPs obtained at 550^{o}C

The composition of FePt NPs prepared at 350 ^{o}C, 550 ^{o}C and 750 ^{o}C was characterized by EDS (Figure S3, Supporting Information), which indicate that all the atomic ratios of Fe and Pt are close to 1:1. For all the samples prepared at the temperatures from 300 ^{o}C to 750 ^{o}C, the compositions of Fe and Pt have no much different from the element input. For one typical example, the elements distribution of the FePt particles obtained at 550 ^{o}C is characterized by the high-angle annular dark field (HAADF) image and by the atomically resolved scanning transmission electron microscopy-EDS (STEM-EDS), which were shown in **Figure 5**. The uniform distribution of Fe (yellow) and Pt (blue) within one FePt particle can be seen clearly. This means that the composition of the synthesized nanoparticles can be easily controlled by the input elements. It can conclude that this one-step solid-phase synthesis is a very nice method to obtain nanoparticles with tailored size and controlled composition only depending on sintering temperatures and elements input.

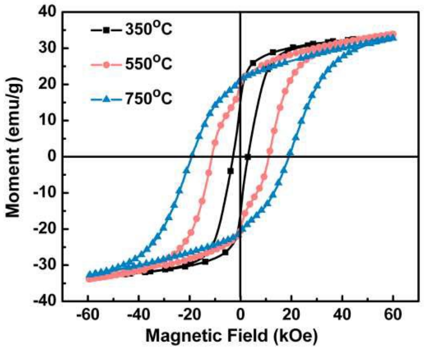

Figure 6. Room temperature hysteresis loops of the FePt NPs prepared at temperatures of 350 °C, 550 °C and 750 °C, respectively

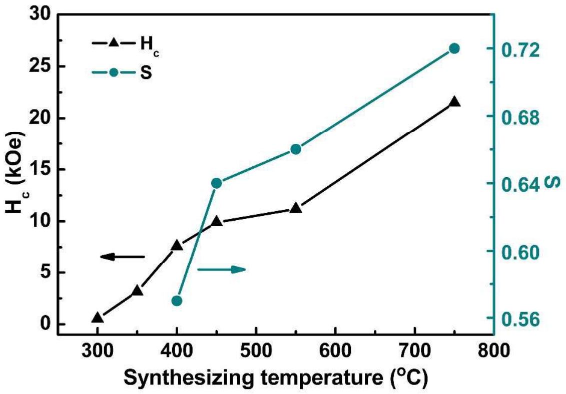

Figure 7. Temperature dependence of coercivity H_c and chemical ordering degree S of the prepared FePt nanoparticles

In order to find out how the sintering temperature influence the magnetic properties of the synthesized FePt NPs, the magnetic hysteresis loops for the samples prepared at 350 °C, 550 °C and 750 °C are shown in **Figure 6**. Samples prepared at 300 °C, 400 °C, 450 °C are shown in Figure S4 (Supporting Information). A magnetic field of 60 kOe is enough to saturate the magnetization. The coercivity H_c dependence on the size and sintering temperatures is also listed in **Table 1** in the supporting information. It shows that the coercivity, H_c, increases with increasing synthesizing temperature. The particles prepared at 300 °C show soft magnetism behavior and has a very small coercivity of 530 Oe, which comes from fcc-FePt phase. And, the 3150 Oe coercivity for the particles obtained at sintering temperature of 350 °C indicates that $L1_0$-FePt phase starts to form. With the further increase of the sintering temperature, H_c becomes larger and larger as plotted in **Figure 7** (also listed in Table 1 in the supporting information). A small kink was observed in the hysteresis loop of the NPs prepared at 400~550 °C, which may due to the presence of the small size superparamagnetic FePt nanoparticles below 2.8 nm.[14] A coercivity value of up to 21.5 kOe has been achieved from the hard magnetic nanoparticles prepared at 750°C. The coercivity is not only influenced by particle size, and it is also associated with chemical ordering. The chemical ordering degree of S was also plotted in Figure 7. The observed increase of coercivity depending on synthesizing temperature can be explained by the increase of the chemical order and the increase of size below the single domain region.

In conclusion, we developed a simple and environmental friendly one-step solid-phase method to synthesize $L1_0$-FePt NPs. This method can realize controlling synthesis both in size and compositions. By sintering a mixture of precursor (Fe and Pt) and NaCl at different temperatures under a reducing atmosphere flow, single crystal FePt NPs with a large mean size range from 6.6 to 15nm can be obtained by only one step. The medium of NaCl particles firstly works as the substrate of nanoparticles nucleation and growth, and then acts as insulation medium preventing coalescence phenomena in higher sintering temperatures. Magnetic analysis shows that the coercivity of the synthesized FePt NPs is strongly dependent on sintering temperatures, which influence both the particle size and chemical ordering degree. Once sintered at temperature up to 350 ^{o}C, the FePt NPs can become room temperature ferromagnets and a coercivity of several thousand Oe can be achieved. When the sintering temperature is up to 750 ^{o}C, the highest H_c of 21.5 kOe can be obtained. This work gives out an environmental friendly synthesis, which may not only be used for synthesis alloy nanoparticles with bimetallic, or polymetallic elements, or metallic oxide nanoparticles, but also can synthesis nanoparticles with high temperature chemically ordered phase.

Acknowledgements

The authors would like to acknowledge the National Basic Research Program of China, under grant no. 2014CB643702; the National Natural Science Foundation of China, under grant no. 51422106, 51401228, 51101168, 61428403; the Key Research Program of the Chinese Academy of Sciences, under grant no. KGCX2-EW-215; the Ningbo City Scientific and Technological Project under grant no. 2012B81001, Scientific and Technological Project of Zhejiang Province under grant no. 2013TD08; and the China Postdoctoral Science Foundation under grant no. 2014M561524 for financial support.

References

---

[1] K. Inomata, T. Sawa, S. Hashimoto, J. Appl. Phys. **1988**, 64, 2537.

[2] a) J. P. Wang, Proc. IEEE **2008**, 96, 1847; b) S. H. Sun, C. B. Murray, D. Weller, L. Folks, A. Moser, Science **2000**, 287, 1989.

[3] a) H. Zeng, J. Li, J. P. Liu, Z. L. Wang, S. H. Sun, Nature **2002**, 420, 395; b) C. B. Rong, D. R. Li, V. Nandwana, N. Poudyal, Y. Ding, Z. L. Wang, H. Zeng, J. P. Liu, Adv. Mater. **2006**, 18, 2984.

[4] a) S. J. Guo, S. H. Sun, J Am Chem Soc **2012**, 134, 2492; b) J. Kim, Y. Lee, S. H. Sun, J. Am. Chem. Soc **2010**, 132, 4996.

[5] a) S. W. Chou, Y. H. Shau, P. C. Wu, Y. S. Yang, D. B. Shieh, C. C. Chen, J. Am. Chem. Soc. **2010**, 132, 13270; b) C. J. Xu, Z. L. Yuan, N. Kohler, J. M. Kim, M. A. Chung, S. H. Sun, J. Am. Chem. Soc. **2009**, 131, 15346.

[6] S. H. Sun, Adv. Mater. **2006**, 18, 393.

[7] a) Y. Tamada, S. Yamamoto, M. Takano, S. Nasu, T. Ono, Appl. Phys. Lett. **2007**, 90; b) S. Yamamoto, Y. Morimoto, T. Ono, M. Takano, Appl Phys Lett **2005**, 87; c) J. M. Kim, C. B. Rong, J. P. Liu, S. H. Sun, Adv. Mater. **2009**, 21, 906.

[8] a) K. Elkins, D. Li, N. Poudyal, V. Nandwana, Z. Q. Jin, K. H. Chen, J. P. Liu, J. Phys. D Appl. Phys. **2005**, 38, 2306; b) D. R. Li, N. Poudyal, V. Nandwana, Z. Q. Jin, K. Elkins, J. P. Liu, J. Appl. Phys. **2006**, 99, 08E911.

[9] a) I. Zafiropoulou, E. Devlin, N. Boukos, D. Niarchos, D. Petridis, V. Tzitzios, Chem. Mater. **2007**, 19, 1898; b) H. B. Wang, P. J. Shang, J. Zhang, M. W. Guo, Y. P. Mu, Q. Li, H. Wang, Chem. Mater. **2013**, 25, 2450.

[10] C. N. He, N. Q. Zhao, J. Mater. Chem. **2012**, 22, 1297.

[11] X. C. Hu, E. Agostinelli, C. Ni, G. C. Hadjipanayis, A. Capobianchi, Green Chem. **2014**, 16, 2292.

[12] B. R. Bian, J. H. He, J. Du, W. X. Xia, J. Zhang, J. P. Liu, W. Li, C. F. Hu, A. Yan, Nanoscale **2015**, 7, 975.

[13] J. A. Christodoulides, P. Farber, M. Daniil, H. Okumura, G. C. Hadjipanayis, V. Skumryev, A. Simopoulos, D. Weller, IEEE T. Magn. **2001**, 37, 1292.

[14] A) D. Weller, A. Moser, L. Folks, M. E. Best, W. Lee, M. F. Toney, M. Schwickert, J. U. Thiele, M. F. Doerner, IEEE T. Magn. **2000**, 36, 10; b) J. P. Liu, JOM-US **2010**, 62, 56.